Solid State Communications 151 (2011) 1314–1317

Contents lists available at SciVerse ScienceDirect

Solid State Communications

journal homepage: www.elsevier.com/locate/ssc

X-ray and electron spectroscopy investigation of the core–shell nanowires of ZnO:Mn

A.A. Guda [a,*], N. Smolentsev [a,b], J. Verbeeck [c], E.M. Kaidashev [d], Y. Zubavichus [e], A.N. Kravtsova [a], O.E. Polozhentsev [a], A.V. Soldatov [a]

[a] Research center for nanoscale structure of matter, Southern Federal University, Rostov-on-Don, 344090, Russia
[b] European Synchrotron Radiation Facility, Grenoble, 38000, France
[c] Electron Microscopy for Materials Science, University of Antwerp, 2020, Antwerp, Belgium
[d] Vorovich Research Institute of Mechanics and Applied Mathematics and Faculty of Physics, Southern Federal University, Rostov-on-Don, 344090, Russia
[e] National Research Center "Kurchatov Institute", Moscow, 123182, Russia

ARTICLE INFO

Article history:
Received 15 June 2011
Accepted 20 June 2011
by E.L. Ivchenko
Available online 28 June 2011

Keywords:
A. Semiconductors
C. EXAFS, NEXAFS, SEXAFS
C. Scanning and transmission electron microscopy
E. Electron energy loss spectroscopy

ABSTRACT

ZnO/ZnO:Mn core–shell nanowires were studied by means of X-ray absorption spectroscopy of the Mn K- and $L_{2,3}$-edges and electron energy loss spectroscopy of the O K-edge. The combination of conventional X-ray and nanofocused electron spectroscopies together with advanced theoretical analysis turned out to be fruitful for the clear identification of the Mn phase in the volume of the core–shell structures. Theoretical simulations of spectra, performed using the full-potential linear augmented plane wave approach, confirm that the shell of the nanowires, grown by the pulsed laser deposition method, is a real dilute magnetic semiconductor with Mn^{2+} atoms at the Zn sites, while the core is pure ZnO.

1. Introduction

ZnO nanofilms and nanowires attract a great deal of attention due to their potential application in spintronics and optoelectronic devices since theoretical prediction of the room-temperature ferromagnetism [1]. Great experimental efforts [2–10] were carried out in the past few years in order to obtain high quality ZnO:Mn samples with room-temperature ferromagnetism which is important for spintronic [5] applications. Nevertheless there are reports in the literature on the room-temperature ferromagnetism of pure ZnO thin films [6], ZnO:Mn nanorods [7], and on the absence of ferromagnetism in Mn doped ZnO alloys [8] and nanoneedles [9]. It was found that doping atoms can form secondary phases, such as Mn_3O_4 in ZnO:Mn annealed nanorods [7], Co clusters in ZnO:Co films prepared by the pulsed laser deposition [9], the so-called embedded clusters [11] or nanoscale clusters [12,13] inside the host lattice. Differences in the atomic structure around Mn atoms result in the observation of the different magnetic properties. Thus, investigation of local atomic and electronic structures of Mn atoms inside the ZnO lattice is of great importance.

X-ray absorption near edge structure (XANES) spectroscopy is sensitive to the atomic and electronic structure around the absorbing atom [14,15]. In the hard X-ray region (e.g. for Mn K-edge), it has sensitivity mostly to the atomic structure, while in the soft X-rays (e.g. for Mn $L_{2,3}$-edges) it probes mostly the electronic structure of Mn atoms. This difference arises from angular momentum sensitivity of XANES. For K-edges XANES spectrum probes p-density of states (DOS), while for $L_{2,3}$-edge transitions to d-DOS are allowed [15]. For 3d-transition metals, d-DOS is strongly localized and multi-electronic transitions influence on XANES spectrum dramatically [15]. 15 nm X-ray focusing was achieved recently using Fresnel zone plates [16]. However, despite this progress, it is still not sufficient to study core–shell nanostructures with shell around 2 nm thickness. Electron spectroscopies have advantage of the sub-nanometer focusing [17]. The electron energy loss spectroscopy (EELS) is complimentary to XANES [18].

ZnO/ZnO:Mn core–shell nanowires were synthesized and characterized previously by means of Raman spectroscopy [19]. In the present work we examine in detail the local atomic structure around Mn atoms and Mn distribution in the nanowires. The Mn $L_{2,3}$-, and the Mn K-edge XANES spectroscopy, EELS at the O K-edge and Mn $L_{2,3}$-edges were used for the determination of

* Corresponding author. Tel.: +7 863 2975 326; fax: +7 863 2901 003.
E-mail addresses: guda_sasha@mail.ru, guda@sfedu.ru (A.A. Guda).

0038-1098/$ – see front matter © 2011 Elsevier Ltd. All rights reserved.
doi:10.1016/j.ssc.2011.06.028

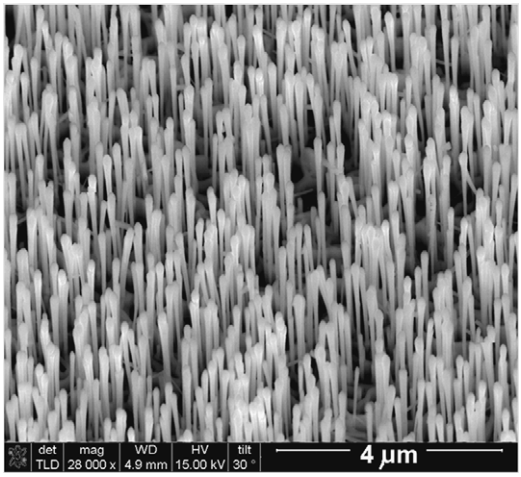

Fig. 1. SEM image of core–shell $Zn_{0.9}Mn_{0.1}O$(shell)/ZnO(core)/Au, 2nm/(11–20) Al_2O_3 nanowires.

the atomic structure in the shell and the core of nanowires. Energy filtered transmission electron microscopy (EFTEM) was used for the element spatial distribution analysis.

2. Experimental details

ZnO/ZnO:Mn core–shell nanowires have been synthesized by deposition of an epitaxial layer of $Zn_{0.9}Mn_{0.1}O$ onto single-crystalline ZnO nanowires by pulsed laser deposition (PLD). ZnO nanowires have been grown by PLD at high pressure argon (100 mbar) on sapphire substrates using Au catalysts [20]. Typically, 12,000 laser pulses with 10 Hz repetition rate were applied for one deposition process and the laser fluence on the target was approximately 2 J/cm^2. The growth temperature was around 830 °C. After the growth of the ZnO nanorods, pulsed laser deposition of ZnO:Mn film (750–1000 laser pulses) was carried out following previous publication [21] by one of us. The deposition process of the ZnO:Mn shell was performed at a temperature of 530 °C in an ambient oxygen pressure of 0.3 mbar. A scanning electron microscopy (SEM) image of the resulting core–shell nanorods is presented in Fig. 1.

Experimental Zn K-edge XANES spectra of ZnO nanorods and bulk crystalline ZnO have been measured in fluorescence mode using a crystal-monochromator Ge(311) and a scintillation detector SC-70 at the "Rigaku" R-XAS Looper spectrometer in Southern Federal University. Experimental Mn K-edge XANES spectra of reference Mn compounds and ZnO/ZnO:Mn core/shell structures have been measured in fluorescence mode using a NaI(Tl) scintillator detector with a photoelectronic multiplier at the synchrotron radiation facility "SIBERIA-2" (Kurchatov Center of Synchrotron Radiation and Nanotechnology, Moscow) [22], due to the very low concentration for laboratory spectrometer.

The Mn $L_{2,3}$- and Zn $L_{2,3}$-absorption spectra were measured under ultra-high vacuum conditions in the Russian–German beamline of the synchrotron BESSY-II (Berlin). Energy resolution at the Mn $L_{2,3}$ edge was better than 0.1 eV. The size of the beam spot was about 30 × 100 µm. The sample was mounted on a conductive tape and the total electron yield (TEY) signal was measured for different photon energy in order to obtain XANES spectrum.

EELS spectra of the O K-edge and Mn $L_{2,3}$ edge were recorded on a Jeol 3000F microscope operating at 300 kV equipped with a Gatan GIF2000 imaging spectrometer. Energy filtered transmission electron microscopy (EFTEM) images were recorded in filtered imaging mode making use of the three window method to obtain elemental maps of O and Mn.

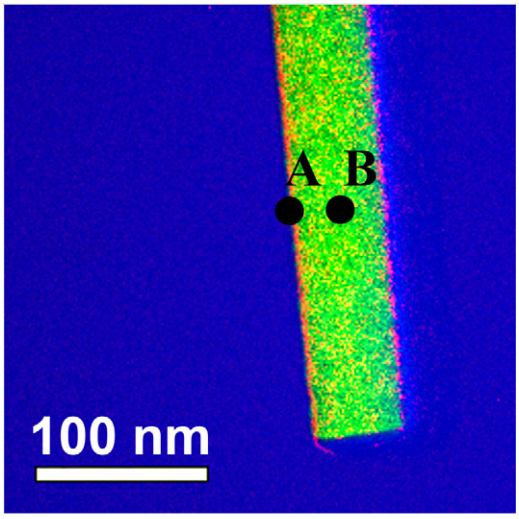

Fig. 2. (Color online). EFTEM combined elemental image (Mn atoms are shown in red color, oxygen atoms are shown in green color) of a single ZnO/ZnO:Mn core–shell nanowire.

3. Calculation details

Spin-polarized electron structure calculations were performed by means of a full-potential linearized augmented plane wave method, implemented in the Wien2k program package [23]. A supercell, composed of 2 × 2 × 2 conventional wurtzite ZnO cells was used to model a 6.25 at.% of Mn defects in ZnO lattice. The generalized gradient approximation within Perdew et al. exchange-correlation functional [24] was used for treatment of the exchange-correlation interactions. K-point convergence was reached within 2000 k-points per ZnO unit cell (that is equal to approximately 250 k-points per 2 × 2 × 2 supercell). Energy convergence in the self-consistent iteration procedure was better 0.1 mRy and force convergence in geometry structure optimization was better 1 mRy · A^{-1}.

4. Results and discussions

Fig. 2 shows a combined O and Mn EFTEM image of a single ZnO:Mn nanowire. The distribution of Mn atoms (red) on the outside of the ZnO wire is clearly visible. The oxygen atoms (green) are homogeneously distributed throughout the core of the nanowire. Letters A and B mark schematically the regions used for EELS measurements.

The XANES spectroscopy was used for subsequent sample characterization. It was found that the Zn $L_{2,3}$-edge spectrum (as well as the Zn K-edge) of ZnO:Mn nanowires resembles closely the spectrum of pure ZnO nanowires, thus indicating good quality of the samples. The Mn $L_{2,3}$ XANES spectra for the ZnO:Mn sample, MnO and Mn_3O_4 reference samples are shown in Fig. 3 (spectra for MnO and Mn_3O_4 are reproduced from the Ref. [25]). Thin films of Mn doped ZnO [26] also exhibit similar Mn $L_{2,3}$ absorption spectrum. Spectrum of the ZnO:Mn sample is very close to MnO. It can be used as a "fingerprint" of the Mn^{2+} configuration, because absorption spectrum changes dramatically when charged state of Mn increases, as can be seen for Mn_3O_4. Observed low-energy pre-edge structure A, which is absent in ZnO:Mn and present in MnO can be attributed to the crystal field effects. Simulations for single Mn^{2+} ion reveal the absence of this peak when the crystal field is switched off. Crystal field with octahedral symmetry causes the peak growth (Fig. 21 in Ref. [27]). Configuration-interaction calculations, performed in [28] also reproduce the differences in spectra for ZnO:Mn and MnO. Since TEY signal originates from a

Table 1
Distances in the first coordination sphere around Mn atom in Zn site, obtained from different theoretical strategies.

	Crystal ZnO	DFT spin-restricted	DFT spin-polarized	XANES fitting
Three lateral oxygens, Å	1.97	1.88	2.01	1.98
One apical oxygen, Å	1.99	1.87	2.02	2.02

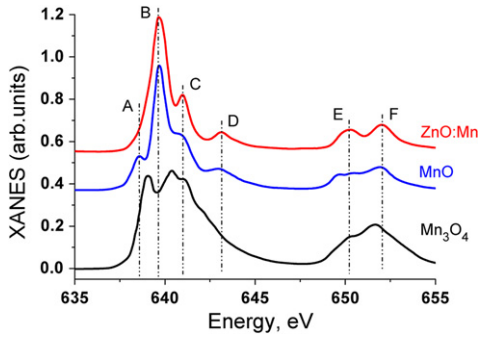

Fig. 3. From up to down: Experimental Mn $L_{2,3}$ XANES spectra of ZnO/ZnO:Mn core–shell nanowires, MnO and Mn_3O_4 (data from Ref. [25]). Spectra are shifted vertically for clarity.

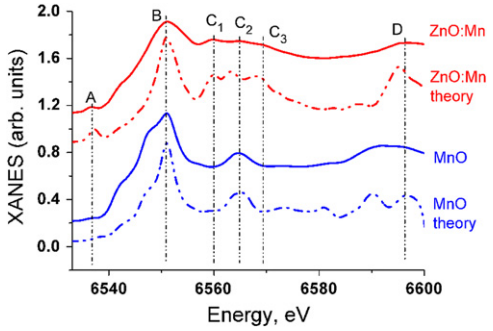

Fig. 4. From up to down: Experimental Mn K-XANES spectra of ZnO/ZnO:Mn core–shell nanowires, calculated spectrum for Mn in Zn site inside ZnO, experimental spectrum for MnO and calculated spectrum for MnO.

depth of approximately 5 nm from the sample surface [15], Mn $L_{2,3}$ XANES probes the surface region of the nanowires, which is Mn-rich as it was shown by EFTEM measurements in Fig. 2. Thus we conclude that most of Mn atoms have 2+ oxidation state in the ZnO:Mn core/shell nanowires.

While Mn $L_{2,3}$ absorption spectra are sensitive to the charge state of the absorbing atom, they are insensitive to the local atomic structure around it. Below we use K-edge absorption spectroscopy for subsequent geometry analysis around Mn atoms. Fig. 4 shows experimental Mn K-edge XANES spectra for the ZnO/ZnO:Mn nanowire sample, the MnO reference and simulations for a Mn in the Zn site model and MnO. Energy positions of labeled peaks were chosen to represent maxima of ZnO:Mn spectrum. Theoretical model, when Mn substitutes Zn has best agreement with experiment among other models when Mn occupies interstitial positions or oxygen site. The differences between MnO and nanowires XANES spectra are more pronounced than in Fig. 3, because X-ray absorption spectra above K-edge are more sensitive to the geometry structure around absorbing atom and usually used for evaluation of structural parameters [29].

Initial parameters of wurtzite ZnO were taken from Ref. [30]. Using $a = b = 3.25$ Å, $c = 5.21$ Å, space group P63mc and atomic coordinates Zn(1/3, 2/3, 0), O(1/3, 2/3, 0.382) in the unit cell one obtains initial values for Zn–O distances in the first coordination sphere: 1.97 Å (for three lateral oxygen atoms in the plane perpendicular to c axis of wurtzite lattice) and 1.99 Å (for

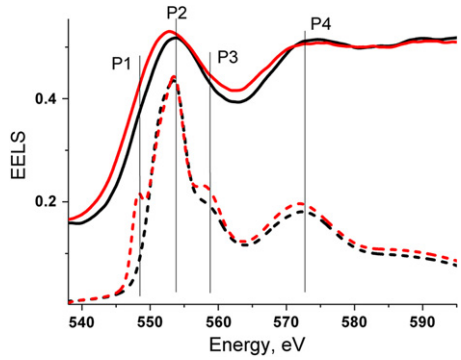

Fig. 5. (Color online). Upper curves are the experimental EELS for A (red line) and B (black line) points on the nanowires from Fig. 2. Bottom curves are the simulated O K-edge EELS spectra for pure ZnO (black line) and ZnO:Mn with Mn in Zn site (red line). Spectra are shifted vertically for clarity.

one apical oxygen atom along the c axis). When Mn substitutes Zn these distances change. Results of the theoretical analysis of these changes are presented in Table 1. We use geometry optimization of the supercell with Mn defect (DFT) and compare it with theoretical fitting of structural parameters using Mn K-edge XANES according Ref. [31] (XANES fitting). Geometry optimization results are greatly affected if magnetization of Mn atoms is taken into account (spin-polarized calculations) or not (spin-restricted calculations).

Geometry optimization within spin unrestricted generalized gradient approximation (DFT spin-polarized in Table 1) is in a good agreement with values, obtained from theoretical simulations of spectrum and subsequent fitting to experiment. The small differences in the distances to the lateral oxygens can be explained by inaccuracies in the exchange-correlation functional for description of 3d metal magnetization.

Intensities of the peaks marked C_1, C_2 and C_3 in Fig. 4 are sensitive to the structural disorder around dopants inside ZnO. Different authors used similar energy region to study the oxygen vacancies in the Co- [32,33] and Mn- [34] doped ZnO. The presence of the oxygen vacancy in the first coordination sphere of absorbing Mn atom changes greatly the relative intensities of the C_1 and C_2, C_3 peaks. For unambiguous conclusions one should use adequate approximation to for spectra simulations. We have simulated first the spectrum for model MnO compound, tested the influence of the supercell size and the potential approximation on the spectrum shape (please look in the supplementary material at doi:10.1016/j.ssc.2011.06.028). Since single Mn substitution defect reproduce well experimental spectrum we can conclude that concentration of O vacancies or Zn interstitials in the Mn local neighborhood is negligible.

Finally, we have used spatially resolved EELS spectroscopy and measured the O K-edge EELS spectra from 2 different regions of the nanowire, marked shell and core (A and B letters at Fig. 2), respectively. This method turned out to be fruitful for analysis of Mn doped ZnO, as shown in Refs. [3,35]. Fig. 5 shows experimental and theoretical calculated spectra for bulk crystalline ZnO and relaxed ZnO:Mn. We used lower value of energy broadening in order to clarify the experimentally observed changes in the intensity of peaks P1–P4. Since O K-edge EELS reflects the unoccupied oxygen p-states, the hybridization of these states with Mn d-states result in the appearance of low-energy levels.

These levels appear as pre-edge peak A in Fig. 4 and pre-edge peak P1 in Fig. 5. The lattice relaxation around Mn defect results in the changes of the P3 and P4 peaks intensities.

For the obtained structural parameters around Mn atom in Zn site the Bader analysis [36,37] of the charge on atoms was performed using the procedure implemented in the Wien2k code. In the $2 \times 2 \times 2$ supercell with one Mn in Zn site average charge on each Zn atom is $+1.2e$, oxygen atom has charge -1.2 and Mn atom has a charge $+1.4$. This results are consistent with previous detailed analysis of ZnO bonding mechanism, performed in [38]. Formal oxidation state of Zn in ZnO is $2+$. Since Bader charges on Zn and Mn atoms are similar one can conclude that when Mn occupies Zn site its charged state can also be attributed to the Mn^{2+}. This was also confirmed by the analysis of the Mn $L_{2,3}$ XANES spectra.

5. Conclusions

In summary, we have used a variety of spectroscopic techniques to investigate the local atomic structure of core/shell ZnO/ZnO:Mn nanowires, prepared by pulsed laser deposition. The combination of surface sensitive Mn $L_{2,3}$ with bulk sensitive Mn K-edge XANES spectroscopy was used for local atomic structure analysis around Mn ions in the ZnO lattice. It was found that the shell of the nanowires contains the majority of Mn atoms, which are found to be substitutional on the Zn sites. Both XANES spectra above Mn $L_{2,3}$ edge and DFT analysis show that Mn atoms are in $2+$ oxidation state. No secondary phases or Mn nanoclusters were observed and the concentration of ZnO-related defects, such as O vacancies and Zn interstitials, is negligible in the Mn local neighborhood. The energy filtered transmission electron microscopy provided the visual observation of the Mn distribution along the core–shell nanowire.

Acknowledgments

We acknowledge the Helmholtz-Zentrum Berlin — Electron storage ring BESSY-II for provision of synchrotron radiation at the Russian–German beamline and financial support. This research was supported by the Russian Ministry to education and science (RPN 2.1.1. 5932 grant and RPN 2.1.1.6758 grant). N.S. and A.G. would like to thank the Russian Ministry of Education for providing the fellowships of President of Russian Federation to study abroad. We would like to thank the UGINFO computer center of Southern federal university for providing the computer time.

References

[1] T. Dietl, H. Ohno, F. Matsukura, J. Cibert, D. Ferrand, Science 287 (2000) 1019–1022.
[2] M. Diaconu, H. Schmidt, H. Hochmuth, M. Lorenz, G. Benndorf, J. Lenzner, D. Spemann, A. Setzer, K.-W. Nielsen, P. Esquinazi, M. Grundmann, Thin Solid Films 486 (2005) 117–121.
[3] P. Sharma, A. Gupta, K.V. Rao, F.J. Owens, R. Sharma, R. Ahuja, J.M.O. Guillen, B. Johansson, G.A. Gehring, Nat Mater 2 (2003) 673–677.
[4] C. Liu, F. Yun, H. Morkoç, Journal of Materials Science: Materials in Electronics 16 (2005) 555–597.
[5] F. Pan, C. Song, X.J. Liu, Y.C. Yang, F. Zeng, Materials Science and Engineering: R: Reports 62 (2008) 1–35.
[6] H. Nguyen Hoa, J. Sakai, V. Brizé, Journal of Physics: Condensed Matter 19 (2007) 036219.
[7] H.B. Wang, H. Wang, C. Zhang, F.J. Yang, C.P. Yang, H.S. Gu, M.J. Zhou, Q. Li, Y. Jiang, Materials Chemistry and Physics 113 (2009) 884–888.
[8] Z. Hua-Wei, E.-W. Shi, Z.-Z. Chen, X.-C. Liu, B. Xiao, Journal of Physics: Condensed Matter 18 (2006) L477.
[9] W. Xiao, Q. Chen, Y. Wu, T. Wu, L. Dai, Materials Chemistry and Physics 123 (2010) 1–4.
[10] Z. Sun, W. Yan, G. Zhang, H. Oyanagi, Z. Wu, Q. Liu, W. Wu, T. Shi, Z. Pan, P. Xu, S. Wei, Physical Review B 77 (2008) 245208.
[11] S. Wei, W. Yan, Z. Sun, Q. Liu, W. Zhong, X. Zhang, H. Oyanagi, Z. Wu, Applied Physics Letters 89 (2006) 121901–121903.
[12] A.A. Guda, S.P. Lau, M.A. Soldatov, N.Yu. Smolentsev, V.L. Mazalova, X.H. Ji, A.V. Soldatov, Journal of Physics: Conference Series 190 (2009) 012136.
[13] R. Larde, E. Talbot, P. Pareige, H. Bieber, G. Schmerber, S. Colis, V.R. Pierron-Bohnes, A. Dinia, Journal of the American Chemical Society 133 (2011) 1451–1458.
[14] J.J. Rehr, R.C. Albers, Reviews of Modern Physics 72 (2000) 621.
[15] F.D. Groot, A. Kotani, Core Level Spectroscopy of Solids, Taylor & Francis CRC Press, 2008.
[16] K. Jefimovs, J. Vila-Comamala, T. Pilvi, J. Raabe, M. Ritala, C. David, Physical Review Letters 99 (2007) 264801.
[17] S.J. Pennycook, M. Varela, A.R. Lupini, M.P. Oxley, M.F. Chisholm, Journal of Electron Microscopy 58 (2009) 87–97.
[18] E. Stavitski, F.M.F. de Groot, Micron 41 (2010) 687–694.
[19] V.E. Kaydashev, E.M. Kaidashev, M. Peres, T. Monteiro, M.R. Correia, N.A. Sobolev, L.C. Alves, N. Franco, E. Alves, Journal of Applied Physics 106 (2009) 093501.
[20] M. Lorenz, E.M. Kaidashev, A. Rahm, T. Nobis, J. Lenzner, G. Wagner, D. Spemann, H. Hochmuth, M. Grundmann, Applied Physics Letters 86 (2005) 143113.
[21] E.M. Kaidashev, M. Lorenz, H. von Wenckstern, A. Rahm, H.C. Semmelhack, K.H. Han, G. Benndorf, C. Bundesmann, H. Hochmuth, M. Grundmann, Applied Physics Letters 82 (2003) 3901–3903.
[22] A.A. Chernyshov, A.A. Veligzhanin, Y.V. Zubavichus, Nuclear Instruments and Methods in Physics Research Section A: Accelerators, Spectrometers, Detectors and Associated Equipment 603 (2009) 95–98.
[23] P. Blaha, K. Schwarz, G.K.H. Madsen, D. Kvasnicka, J. Luitz, WIEN2k, An augmented plane wave + local orbitals program for calculating crystal properties, Karlheinz Schwarz, Techn. Universitat Wien, 2001.
[24] J.P. Perdew, S. Burke, M. Ernzerhof, Physical Review Letters 77 (1996) 3865–3868.
[25] B. Gilbert, B.H. Frazer, A. Belz, P.G. Conrad, K.H. Nealson, D. Haskel, J.C. Lang, G. Srajer, G.D. Stasio, Journal of Physical Chemistry A 107 (2003) 2839–2847.
[26] J.-H. Guo, A. Gupta, P. Sharma, K.V. Rao, M.A. Marcus, C.L. Dong, J.M.O. Guillen, S.M. Butorin, M. Mattesini, P.A. Glans, K.E. Smith, C.L. Chang, R. Ahuja, Journal of Physics: Condensed Matter 19 (2007) 172202.
[27] F.D. Groot, Journal of Electron Spectroscopy and Related Phenomena 67 (1994) 529–622.
[28] I. Tanaka, F. Oba, Journal of Physics: Condensed Matter 20 (2008) 064215.
[29] G. Smolentsev, A.V. Soldatov, M.C. Feiters, Physical Review B (2007) 144106.
[30] U. Ozgur, Y.I. Alivov, C. Liu, A. Teke, M.A. Reshchikov, S. Dogan, V. Avrutin, S.-J. Cho, H. Morkoç, Journal of Applied Physics 98 (2005) 041301.
[31] N. Smolentsev, A.V. Soldatov, G. Smolentsev, S.Q. Wei, Solid State Communications 149 (2009) 1803–1806.
[32] T. Shi, S. Zhu, Z. Sun, S. Wei, W. Liu, Applied Physics Letters 90 (2007) 102108.
[33] X.-C. Liu, E.-W. Shi, Z.-Z. Chen, B.-Y. Chen, T. Zhang, L.-X. Song, K.-J. Zhou, M.-Q. Cui, W.-S. Yan, Z. Xie, B. He, S.-Q. Wei, Journal of Physics: Condensed Matter 20 (2008) 025208.
[34] C. Guglieri, E. Céspedes, C. Prieto, J. Chaboy, Journal of Physics: Condensed Matter 23 (2011) 206006.
[35] H.K. Schmid, W. Mader, Micron 37 (2006) 426–432.
[36] R.F.W. Bader, Atom in Molecule—A Quantum Theory, Clarendon Press, Oxford, UK, 1990.
[37] R.F.W. Bader, Chem. Rev. 91 (1991) 893.
[38] G.C. Zhou, L.Z. Sun, X.L. Zhong, X. Chen, L. Wei, J.B. Wang, Physics Letters A 368 (2007) 112–116.